COBEM 2023 27TH INTERNATIONAL CONGRESS OF MECHANICAL ENGENEERING

ABCM Brazilian Society of Mechanical Sciences and Engineering
27th ABCM International Congress of Mechanical Engineering
December 04-08, 2023, Florianópolis-SC, Brazil

COB-2023-0168
A COMPARATIVE STUDY ON THE RADIATIVE HEAT TRANSFER FOR HYPERSONIC NONEQUILIBRIUM FLOWS OVER A CYLINDER

Farney Coutinho Moreira
Instituto Tecnológico de Aeronáutica, São José dos Campos, SP, 12228-900, Brazil
farney.coutinho@gmail.com

Deborah A. Levin
Shubham Thirani
University of Illinois at Urbana-Champaign, Urbana-Champaign, Illinois, 61801, USA
deblevin@illinois.edu
thirani2@illinois.edu

William Roberto Wolf
University of Campinas, UNICAMP, Campinas, SP, 13083-860, Brazil
wolf@fem.unicamp.br

João Luiz F. Azevedo
Instituto de Aeronáutica e Espaço, São José dos Campos, SP, 12228-904, Brazil
joaoluiz.azevedo@gmail.com

Abstract. *Hypersonic flow over a cylinder is modeled using the finite volume method to solve the Navier-Stokes equations, including Park's two-temperature model for chemical dissociation. The main focus of this work is to carry out a comparative analysis of the thermodynamic nonequilibrium properties along the flow stagnation line, and obtain the infrared spectrum of radiative heat flux at the stagnation point of the cylinder using a line-by-line approach. The spectrum of radiative heat flux at the stagnation point of the cylinder are obtained using NEQAIR numerical code, considerig the NEQAIR and HITRAN transitions. In hypersonic flow conditions, it is possible to observe the occurrence of thermodynamic nonequilibrium through the magnitude difference of the translational-rotational and vibrational-electronic temperature modes inside the shock layer forming upstream of the cylinder. Analyses of the thermodynamic nonequilibrium effects are performed, considering the excitation state of the temperature modes, in addition to the chemical effects of dissociation and exchange of molecules and atoms present in the mixture.*

Keywords: *Thermodynamic non-equilibrium, hypersonic flow, thermal radiation, infrared spectra*

1. INTRODUCTION

The study of hypersonic flows in thermodynamic and chemical nonequilibrium state over simple geometric configurations such as a cylinder are essential to test numerical models and validate computational simulations of high physical complexity, as typically observed in flows over capsules during atmospheric re-entry procedures. The geometric configuration of a cylinder is widely used for this purpose, and has a large number of publications available in the literature (Karpuzcu *et al.*, 2023; Daniel *et al.*, 2023).

In the present work, a study of the flow properties along the stagnation line is carried out. In this study, the geometry of a cylinder is considered to simulate hypersonic flows in thermodynamic nonequilibrium state. To carry out the thermodynamic analysis, the results are obtained with the improved numerical tool used in this research, developed from the LeMANS (Scalabrin, 2007) code. The detailed spectra of radiative heat flux at the cylinder stagnation point is obtained using a line-by-line approach with the NEQAIR numerical tool (Cruden and Brandis, 2019).

An overall view of geometrical details of the cylinder and domain boundary is presented in Fig. 1(a), while Fig. 1(b) shows mesh used in the numerical simulations carried out in the present work. The geometry and freestream conditions used in this work are taken from the experiments of Yanes and Austin (2019), with Mach number, velocity, static temperature and density values of 7.2, $3,950$ m/s in the x direction, 752 K, and $3.78 \times 10^{-3} kg/m^3$, respectively. The cylinder was modeled with a radius of 15.88 mm and an isothermal wall at 300 K. Computations are performed considering a free stream mole fraction with 0.79 of molecular nitrogen, N_2, and with 0.21 of molecular oxygen, O_2.

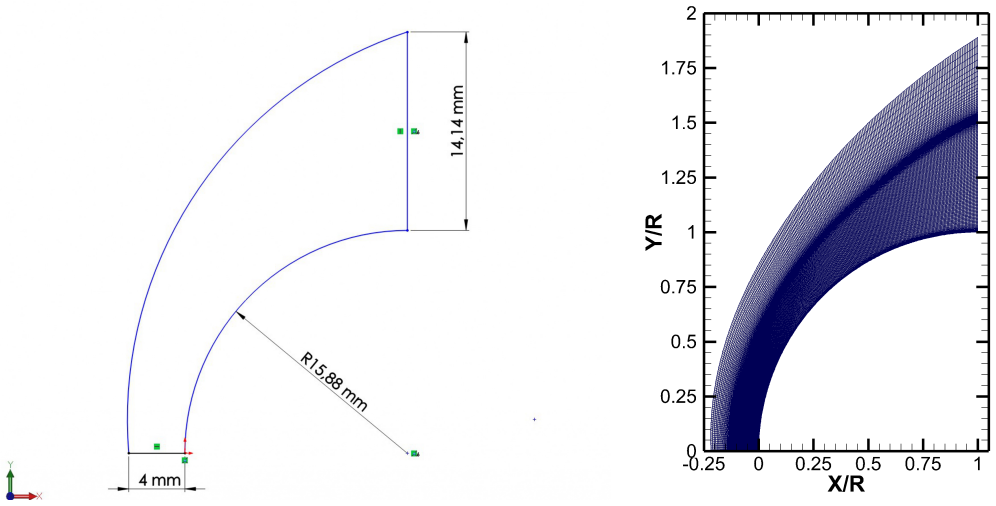

(a) Cylinder geometry with dimensions (b) Computational mesh

Figure 1. 2D view of cylinder geometry and mesh.

2. THEORETICAL FORMULATION

2.1 General Considerations

Hypersonic flows in thermodynamic nonequilibrium state, typically observed in atmospheric re-entry conditions, are subject to distinct flow regimes that vary as a function of the gas density and, thus, that depend on the altitude in the atmosphere. In the last phase of reentry, where density is sufficiently high, no-slip occurs on the vehicle surface. This behavior leads to shear stresses as defined for the flow in a continuous medium. The dimensionless parameter that defines the flow as continuum or rarefied is the Knudsen number, which can be written as

$$K_n = \frac{\lambda}{L} \, . \tag{1}$$

In this expression, the characteristic length scale, L, is a representative measure of the dimension of the fluid-immersed object. For the specific case of a reentry capsule, the outer diameter, or the outer radius, is typically used. The λ parameter is defined as the mean free path, *i.e.*, the average distance traveled by a fluid molecule between successive collisions. Through some mathematical manipulations, it is possible to rewrite the Knudsen number as a function of the Mach and Reynolds numbers (Alladadi *et al.*, 2013) as

$$K_n = \sqrt{\gamma \frac{\pi}{2}} \, \frac{M}{Re} \, . \tag{2}$$

Here, γ represents the ratio of specific heats, M is the Mach number and Re is the Reynolds number. The flow is considered continuum for Knudsen numbers up to $K_n = 0.1$. In this flow regime, the physical problem can be mathematically modeled by the Navier-Stokes equations. The so-called transition regime typically occurs with a Knudsen number ranging from $0.1 < K_n < 1$, and this type of flow should be solved through the kinetic theory of gases, mathematically described by the Burnett equation (Agarwal *et al.*, 2001). For Knudsen numbers $K_n > 1$, the flow becomes rarefied, also called free molecular flow, and statistical approaches that take into account binary collision models are required. The most widely used method for treating phenomena that occur in this last flow regime is the direct simulation Monte Carlo (DSMC) method (Bird, 1994).

In the simulations addressed in the present work, the flows are modeled as continuum since we expect the Knudsen numbers to be of order 10^{-3}. Hence, the Navier-Stokes equations constitute an accurate model for the present high-enthalpy continuum flows. These equations are solved using Park's two-temperature model to account for thermodynamic nonequilibrium and weak ionization effects (Park, 1988). Hence, it is assumed that the rotational and translational energy modes of all species can be described by a single temperature, T_{tr}, and that the vibrational energy mode of all species plus the electron energy can also be described by a single temperature, T_{ve} (Scalabrin, 2007; Martin *et al.*, 2012).

2.2 Conservation Equations and Related Models

Through the Boltzmann equation and the Chapman-Enskog theory (Bobylev, 1982), it is possible to obtain the system of conservation equations for transport of mass, momentum and energy, which are herein referred to as the Navier-Stokes

equations. Here, this system of conservation equations contains a source term that represents chemical reactions including dissociation and ionization under thermodynamic nonequilibrium.

$$\frac{\partial Q}{\partial t} + \frac{\partial (F_j - F_{v_j})}{\partial x_j} = S_{cv} \ , \tag{3}$$

where Q represents the vector of conserved variables and it is defined as

$$Q = \left\{ \begin{array}{ccccccc} \rho_1 & \dots & \rho_N & \rho u_i & E & E_{ve} \end{array} \right\}^T . \tag{4}$$

In the previous equations, index notation has been used and repeated indices imply summation while a free index represents a vectorial equation. In the vector of conserved variables, the terms ρ_1, ..., ρ_N represent the densities of the N chemical species present in the gas mixture. The macroscopic flow velocity components are represented by u_i, the total energy per unit volume is described by E, and the electronic vibrational energy per unit volume of the mixture is represented by E_{ve}.

The components in the j-th direction of the inviscid, F_j, and viscous, F_{v_j}, flux terms are defined as

$$F_j = \left\{ \begin{array}{c} \rho_1 u_j \\ \vdots \\ \rho_N u_j \\ \rho u_i u_j + p\delta_{ij} \\ (E+p)u_j \\ E_{ve} u_j \end{array} \right\} \quad \text{and} \quad F_{v_j} = \left\{ \begin{array}{c} -J_{1,j} \\ \vdots \\ -J_{N,j} \\ \tau_{ij} \\ \tau_{ij} u_i - (q_{tr,j} + q_{ve,j}) - \sum (J_{s,j} h_s) \\ -q_{ve,j} - \sum (J_{s,j} e_{ve,s}) \end{array} \right\} . \tag{5}$$

In the above equations, the p variable represents the mixture pressure and δ_{ij} is the Kronecker delta. According to Fick's law, the diffusion flux of the s-th chemical species in the j-th direction is represented by $J_{s,j} = \rho D_s \frac{\partial Y_s}{\partial x_j}$, and the viscous stress tensor components are defined by τ_{ij}. Here, D_s and Y_s represent the diffusion coefficient and molar fraction of species s, respectively. The thermal flux from translational-rotational energy in the j-th direction is given by $q_{tr,j}$ while $q_{ve,j}$ represents the thermal flux component from electronic-vibrational energy in the j-th direction. Moreover, h_s represents the enthalpy of the s-th chemical species.

The pressure is calculated assuming that each species can be modeled using an ideal gas relation and Dalton's law of partial pressures (Gillespie, 1930)

$$p = \sum_{s=1}^{N} \rho_s \frac{R}{M_s} T_{tr} + \rho_e \frac{R}{M_e} T_{ve} \ , \tag{6}$$

where R is the universal gas constant, T_{tr} is the temperature of translational and rotational modes, T_{ve} is the temperature of vibrational and electronic modes, ρ_s and M_s are the density and molecular weights of the individual chemical species, respectively, ρ_e is the electronic density and M_e is the electronic molecular weight.

The viscous stress tensor for a Newtonian fluid is defined as

$$\tau_{ij} = \mu \left(\frac{\partial u_i}{\partial x_j} + \frac{\partial u_j}{\partial x_i} \right) - \left(\frac{2}{3}\mu - \beta \right) \frac{\partial u_k}{\partial x_k} \delta_{ij} \ , \tag{7}$$

where μ is the shear viscosity and β is the bulk viscosity. Through Stokes' hypothesis, we assume that $\beta = 0$ (Blottner *et al.*, 1971; Nompelis *et al.*, 2009). The bulk viscosity contributes to the dilatational term appearing in the normal stresses and arises from the exchange of momentum between colliding molecules and their internal degrees of freedom. Therefore, one could expect that the momentum exchange across the strong shock waves observed in the present calculation procedure could be directly impacted by this parameter, especially if flows containing carbon dioxide were to be considered. Recent estimation models of bulk viscosity for ideal gases under different temperature ranges are provided in Ref. (Cramer, 2012; Sharma and Kumar, 2019). In general, these models are designed for lower temperatures than those found in the present flows. Moreover, since this is still a topic of investigation, Stokes' hypothesis is assumed in the present work in order to avoid inaccuracies in the evaluation of the bulk viscosity and because we are primarily concerned with reentry to the Earth atmosphere in the present case.

The convective heat fluxes are modeled according to Fourier's law as

$$q_{tr,j} = -k_{tr} \frac{\partial T_{tr}}{\partial x_j} \quad \text{and} \quad q_{ve,j} = -k_{ve} \frac{\partial T_{ve}}{\partial x_j} \ . \tag{8}$$

The thermal conductivity of the mixture for each energy mode is calculated using the approach proposed by Vincenti and Kruger (1982). Hence, the conductivity of the translational-rotational and vibrational-electronic modes are computed,

respectively, as

$$k_{tr,s} = \frac{5}{2}\mu_s Cv_{tr,s} + \mu_s Cv_{ve,s} \tag{9}$$

and

$$k_{ve,s} = \mu_s Cv_{ve,s} \; . \tag{10}$$

Here, $Cv_{tr,s}$ is the constant volume specific heat related to translational-rotational temperature and $Cv_{ve,s}$ is the constant volume specific heat related to vibrational-electronic temperature for the s-th chemical species. The mixture transport properties are modeled using Wilke's semi-empirical mixing rule (Wilke, 1950) as

$$\mu = \sum_s \frac{Y_s \mu_s}{\phi_s} \; , \tag{11}$$

and

$$k = \sum_s \frac{Y_s k_s}{\phi_s} \; , \tag{12}$$

The μ_s and k_s parameters represent the dynamic viscosity and thermal conductivity coefficients for the individual s-th species. The ϕ_s term is calculated using

$$\phi_s = \sum_r Y_r \frac{\left[1 + \sqrt{\frac{\mu_s}{\mu_r}} \left(\frac{M_r}{M_s}\right)^{1/4}\right]^2}{\sqrt{8\left(1 + \frac{M_s}{M_r}\right)}} \; . \tag{13}$$

In the equation above, μ_r and M_r are the viscosity coefficient and molecular weight, respectively, of species r involved in the binary collision with species s. These values can be found in Ref. (Scalabrin, 2007).

In Eq. (3), the S_{cv} source term represents the rates of mass production of species during chemical reactions. This term can be written as

$$S_{cv} = \left\{ \; \dot{\omega}_1 \quad \ldots \quad \dot{\omega}_N \quad 0 \quad 0 \quad 0 \quad 0 \quad \dot{\omega}_v \; \right\}^T \; , \tag{14}$$

where $\dot{\omega}_v$ is the vibrational energy source term, and $\dot{\omega}_1$, ..., $\dot{\omega}_N$ represent, respectively, the mass production rates of all N species due to the chemical reactions.

2.3 Chemical Species

Phenomena associated with dissociation and ionization caused by high-enthalpy flows, typically encountered in hypersonic conditions and atmospheric entry, will determine the chemical species present in the mixture. Some chemical models have been developed and are used to represent these phenomena according to the complexity of the flow physics involved and their chemical reactions (Gnoffo *et al.*, 1989). The information in Table 1 indicates the chemical species that are included in the chemical species model used for the present simulations. The model is referred to as the 5-species model in the paper.

Table 1. Chemical species model for the air used in the present work.

MODEL (NUMBER OF SPECIES)	SPECIES
5	N_2, O_2, N, O, NO

2.4 Model of Chemical Reactions

For all previous models, the chemical reactions of dissociation and ionization can be represented by the following equation

$$\sum \alpha_{rs} \rightleftharpoons \sum \beta_{rs} \quad . \tag{15}$$

Here, s represents the chemical species, and α_{rs} and β_{rs} are the stoichiometric coefficients of the reagents and products, respectively. The reactions are written such that the right arrow represents an endothermic reaction. The rate of chemical production of the s-th species is given by

$$\dot{\omega}_s = M_s \sum_{r=1}^{nr} (\beta_{rs} - \alpha_{rs}) \left[k_{fr} \prod_{s=1}^{N} \left(\frac{\rho_s}{M_s} \right)^{\alpha_{rs}} - k_{br} \prod_{s=1}^{N} \left(\frac{\rho_s}{M_s} \right)^{\beta_{rs}} \right] \quad , \tag{16}$$

where k_{fr} and k_{br} are the forward and backward reaction rates. The latter depends on the equilibrium constant (Park, 1993), k_{eq}, as

$$k_{br} = \frac{k_{fr}\,(T_c)}{k_{eq}\,(T_c)} \quad , \tag{17}$$

where the values of $k_{eq}\,(T_c)$ are obtained by curve fits as follows

$$k_{eq} = \exp\left[A_1 \left(\frac{T_c}{10^4} \right) + A_2 + A_3 \ln \left(\frac{10^4}{T_c} \right) + A_4 \left(\frac{10^4}{T_c} \right) + A_5 \left(\frac{10^4}{T_c} \right)^2 \right] \quad . \tag{18}$$

The A_1, A_2, A_3, A_4 and A_5 coefficients are functions of the flow particle number density within the range of the data tabulated in Ref. (Park, 1989). For number densities outside the range available, the tabulated values for the maximum and minimum number densities are used accordingly.

Under conditions of chemical nonequilibrium, it is reasonable to assume that the order of magnitude of flow and chemical reaction characteristic timescales are comparable. Thus, models that consider a finite rate of chemical reactions are appropriate to consider nonequilibrium effects. The two-temperature model proposed by Park (1989) is widely used due to its simplicity. This model includes the effects of chemical nonequilibrium in the calculations of dissociation rates using a control temperature, T_c, according to

$$T_c = T_{tr}^a T_{ve}^b \, . \tag{19}$$

In this equation, T_{tr} is the translational-rotational temperature mode and T_{ve} is the vibrational-electronic temperature mode. Constants a and b define the nonequilibrium weight factor that controls the energy transfer between dissociation and ionization reactions. The dissociation reactions are controlled by a combination of the translational-rotational and vibrational-electronic temperatures to account for the fact that vibrationally excited molecules are more likely to dissociate (Park, 1988).

Niu *et al.* (2018) present a thorough analysis in terms of the nonequilibrium weight factor considering $a = b = 0.5$, and $a = 0.7$ and $b = 0.3$, for different chemical models. It is shown that the weight factor has an important role on the distribution of the vibrational-electronic temperature in the nonequilibrium process. Here, we use the standard values $a = b = 0.5$. The previous reference shows that this selection leads to good comparisons with experimental results obtained for a blunt body flow in terms of spectral intensity.

In Eq. 16, the forward reaction rates are calculated using Arrhenius curve fits as

$$k_{fr} = A\, T_c^{\eta_k} \exp\left(-\frac{\theta_r}{T_c} \right) \quad , \tag{20}$$

where A is the pre-exponential factor, η_k is the temperature dependence, and θ_r is the activation energy. The forward chemical kinetic rate coefficients used in this work are those proposed by Park (1993).

2.5 One-Dimensional Tangent Slab Approximation

The radiative intensity, I_λ, is defined as the radiative energy per unit solid angle and per unit area normal to an intensity ray. This intensity can be attenuated and augmented through emitting and absorbing media and can be described in differential form by the one-dimensional equation of radiative transfer as given as

$$\frac{dI_\lambda(\theta)}{dx} = -\kappa_\lambda I_\lambda(\theta) + \epsilon_\lambda \quad . \tag{21}$$

where ϵ_λ and κ_λ are the emission and absorption coefficients, respectively. The tangent slab (TS) approximation is one of the basic methods to solve the radiative transport equation (RTE) for a one-dimensional gas media. The spectral radiative heat flux, $q_R(\tau_\lambda)$, which is of interest for heat transfer applications, is written as (Modest, 2003)

$$q_R(\tau_\lambda) = \int_0^{2\pi} \int_0^{\pi} I_\lambda(\theta) cos\theta sin\theta d\theta d\psi \quad . \tag{22}$$

where $\tau_\lambda = \int_0^l \kappa_\lambda ds$ is the optical thickness. The final form to obtain $q_R(\tau_\lambda)$ may be written in terms of the second and third order exponential integrals as,

$$q_R(\tau_\lambda) = 2\pi \left[I_{b1} E_3(\tau_\lambda) - I_{b2} E_3(\tau_{\lambda L} - \tau_\lambda) \right] + 2\pi \left[\int_0^{\tau_\lambda} S_c(\tau_\lambda^{'}) E_2(\tau_\lambda - \tau_\lambda^{'}) d\tau_\lambda^{'} - \int_{\tau_\lambda}^{\tau_{\lambda L}} S_c(\tau_\lambda^{'}) E_2(\tau_\lambda^{'} - \tau_\lambda) d\tau_\lambda^{'} \right] \tag{23}$$

where I_{b1} and I_{b2} are the blackbody intensities at the two wall boundaries. Detailed derivations to solve the radiative heat flux (q_R) and the incident radiative intensity ($G_\lambda = \int_{4\pi} I_\lambda d\Omega$) for the parallel plate media are discussed in Ref. (Modest, 2003). Under radiative equilibrium conditions without scattering the source term, S_c, is defined as the blackbody function. However, for non-equilibrium conditions, local emission and absorption coefficients must be calculated individually for each cell condition, leading to $S_{c\lambda} = \epsilon_\lambda / \kappa_\lambda$. The radiative energy change in a cell is then calculated by

$$\nabla \cdot q_R(\tau_\lambda) = \frac{\Delta q_R(\tau_\lambda)}{\Delta x} \quad . \tag{24}$$

where Δx is the cell thickness.

3. NUMERICAL FORMULATION

The Navier-Stokes equations are solved using the LeMANS parallel code developed at University of Michigan (Scalabrin, 2007; Martin *et al.*, 2012). The solver employs the finite volume method with a cell-centered approach. In this work, the flows are computed using meshes solely composed of quadrilaterals in order to better resolve the boundary layers and shock waves present in hypersonic flows.

The inviscid fluxes across cell faces are discretized using a modified version of the Steger-Warming flux vector splitting scheme (MacCormack and Candler, 1989) which is less dissipative and yields better results along boundary layers. The method switches to the original Steger-Warming scheme (Steger and Warming, 1981) at shock waves by using a pressure switch. A second-order reconstruction of the inviscid fluxes is implemented as discussed in Ref. (Scalabrin, 2007). The viscous fluxes are calculated using a second-order centered scheme that combines properties at cell centers and at the nodes. The property values at the nodes are calculated using a simple average of the cell values that share the node. The use of this method increases the stencil employed in the derivative calculations in order to avoid loss of accuracy when using unstructured meshes. No-slip velocity boundary conditions with catalytic isothermal walls are applied along the solid surfaces for the calculations discussed in the present work.

The spatial discretization of the source term is the same as that used to calculate the viscous flux terms. The values of properties on the left and right sides of a volume face are obtained using the values on the centroid of the respective volume and also the values of properties on the nodes that make up the control volume (Jawahar and Kamath, 2000). Forward and backward chemical reaction rates can achieve large values depending on the control volume temperature, especially for low equilibrium constant values, k_{eq} (Park, 1988). Another numerical problem associated with the source term of chemical reactions is related to the density of chemical species, which needs to be positive. Negative values of densities of chemical species cause the source terms to change sign, which leads to numerical instabilities. The problem arises from the fact that, during the convergence process, and since some of those densities, at a given control volume, can be very small, the calculation procedure might yield negative values to the density of some species. In order to overcome any problems in the calculation of source terms, chemical reaction rates are numerically obtained using a modified temperature as discussed in Ref. (Scalabrin, 2007).

Numerical instabilities may also appear with the use of explicit methods for time integration of the Navier-Stokes equations including source terms with chemical reactions. In such cases, the time step restriction arising from numerical stiffness does not allow an acceptable iteration time for achieving solution convergence (Hirsch, 2007). Since we sought steady state flow solutions, an alternative to avoid this type of problem is to use implicit schemes for time integration of the equations. This approach improves efficiency and robustness, allowing larger time steps while avoiding the growth of numerical instabilities. In this work, the time integration is performed using a line implicit method (Venkatakrishnan, 1995).

The spectrum of radiative heat flux at the stagnation point of the cylinder are obtained using Nonequilibrium Air Radiation (NEQAIR) numerical code. NEQAIR is a line-by-line radiation code developed at NASA Ames (Cruden and Brandis, 2019). It computes the emission and absorption spectra along a line-of-sight for atomic species, molecular species, electronic band systems, and infrared band systems. Radiative heating rate is determined using a tangent slab

assumption (Cruden and Brandis, 2019). Individual electronic transitions are evaluated for atomic and molecular species. The code can model the bound-free and free-free continuum radiation caused by interactions of electrons with neutral and ionized atomic species. The external inputs required by NEQAIR are the nonequilibrium temperatures modes and species number densities along a line-of-sight. In the current implementation, these data are received from DSMC code.

4. RESULTS

4.1 Flow Conditions and Mesh Considerations

In this section, results of hypersonic flow calculations over the cylinder geometry are presented. In order to validate the numerical model, nonequilibrium properties of the gas mixture along the flow stagnation line and the scanned spectra of radiative heat flux at the stagnation point in the frontal region of the cylinder is calculated. The flow conditions are presented in Table 2.

Table 2. Flow configurations investigated in the present work.

$\rho_\infty(kg/m^3)$	$T_\infty(K)$	$T_w(K)$	$U_\infty(m/s)$	M_∞	Re_∞	Kn_∞
3.78×10^{-3}	752	300	3,950	7.19	6.3×10^3	1.68×10^{-3}

In Table 2, ρ_∞ is the freestream density of the flow, T_∞ is the freestream temperature, T_w is the temperature of the surface of the capsule, U_∞ is the flow speed, M_∞ is the freestream Mach number, Re_∞ is the reference Reynolds number and Kn_∞ is the freestream Knudsen number of the flow.

Numerical simulations are performed using 96 Intel Xeon E5-2680v2 2.8 GHz cores. The mesh used in the simulations is composed exclusively of quadrilaterals to better resolve the shock waves and boundary layers in the present flows and to improve the quality of results along the vehicle surface. The convective heat flux calculations are very sensitive to the size of the mesh cells close to the wall. According to a study carried out and published by the authors Moreira *et al.* (2021), for hypersonic flows with high Mach number, the cell Reynolds numbers (Re_{cell}) must be, at most, around 1.0 for better capture of the heat flux at the surface. Here, the cell Reynolds number is defined as $Re_{cell} = Re\,\Delta n/R$, and Δn refers to the smallest normal grid distance on the wall. The number of cells is keep constant with 180 control volumes along the wall-normal direction, and 200 cells along the streamwise direction. Simulations performed are run with 96 cores, and faster convergence was achieved in about 15,000 iterations ($\approx$ 13 h). An overview of the computational mesh with refinement in the shock wave region employed in the CFD simulations is presented in Fig. 1(b).

4.2 Thermodynamic Nonequilibrium Effects

Contours of Mach number are presented in Fig. 2(a). We can observe that the bow shock wave forms close to the stagnation point, generating a thin shock layer. Behind the shock wave, the Mach number is considerably reduced, except at the end of the computational domain where an expansion is observed. In Fig. 2(b) we can clearly observe the formation of a region of thermodynamic nonequilibrium through the contours of the ratio between the temperature modes T_{tr}/T_{ve}. The thermodynamic nonequilibrium region is more intense and thinner near the flow stagnation line, and becomes thicker and less intense as it approaches the expansion region at the flow exit.

4.3 Infrared Radiative Spectra

The modeling of the high temperature air chemistry in hypersonic flows is a complicated problem. The strongly-coupled processes include excitation of the internal energy modes, molecular dissociation, ionization and radiation of the atoms and molecules. Previous radiation modeling efforts of hypersonic air flow shows that nitric oxide (NO) is the dominant radiating species in the ultraviolet and infrared bands (Li *et al.*, 2012). In this work, a comparison of the spectra of NO in the infrared (IR) band is performed using the NEQAIR code. To carry out this comparative study, we are considering two different databases, the NEQAIR equations and the HITRAN database (Rothman, 2021).

Figure 3(a) presents the specific intensity spectra of the radiative heat flux through the infrared band for NO. To obtain the spectrum, the properties along the flow stagnation line are considered, with a total of 198 slabs up to the stagnation point on the cylinder surface. It is possible to observe that, under the analyzed conditions, the main peak of specific intensity occurs at the approximate wavelength of $\lambda = 5.1\mu m$ of the infrared band. The radiative intensity spectrum considering the NEQAIR equations has a greater magnitude than the one observed considering the HITRAN equations. It must be emphasized that the transitions that exist in HITRAN are a mixture of calculated and experimental data, while NEQAIR considers only calculated transitions. Often the experimentally determined values are more accurate than the calculated ones, and vice versa. The calculated values have certain advantages, for example providing a more complete set. But the experimental ones still are usually more accurate.

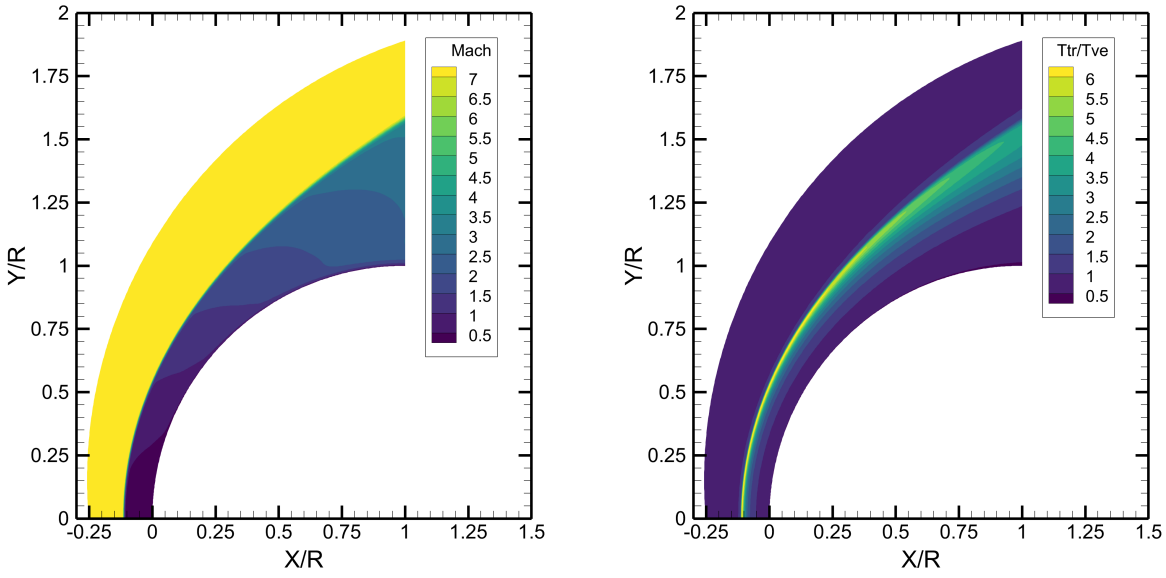

(a) Mach number contours (b) Temperature modes ratio contours

Figure 2. Mach number and temperature mode ratio contours.

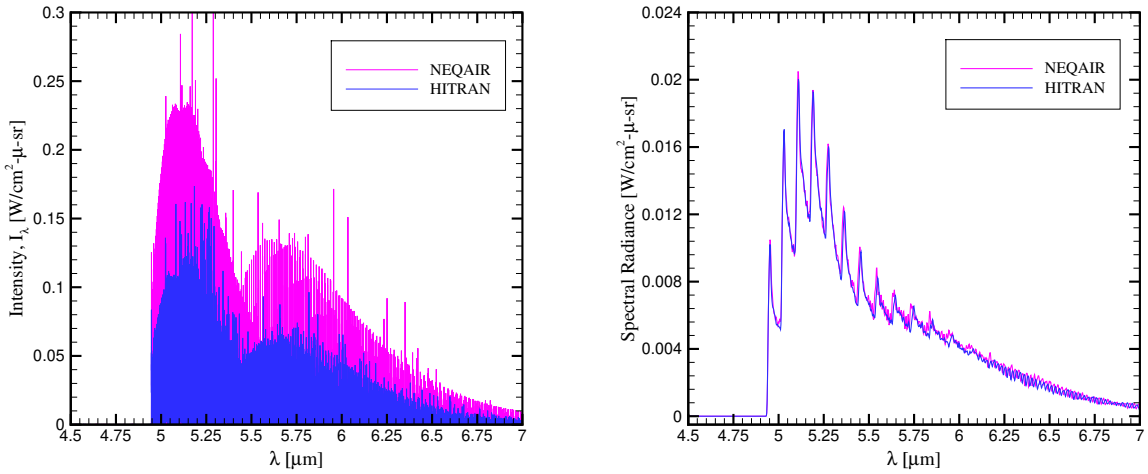

(a) Specific Intensity (b) Scanned Spectra

Figure 3. Line-of-sight calculation for NO using NEQAIR and HITRAN database.

Figure 3(b) presents the results for the scanned spectra through the spectral radiance. We can observe through the scanned spectrum that there is no significant variation between the results obtained considering the NEQAIR and HITRAN databases. We can observe the main peak occurring at the wavelength of $5.1\mu m$, with the incidence of other three adjacent peaks at the wavelengths of $5.19\mu m$, $5.03\mu m$ and $5.27\mu m$, respectively.

The results concerning the scanned spectra reveal a notable similarity when considering both databases, NEQAIR and HITRAN. However, when we examine the results related to specific intensity, it becomes evident that HITRAN stands out, presenting a superior resolution as it covers a much broader range of bands and transitions between energy levels in the NO molecule compared to the NEQAIR database.

5. CONCLUSIONS

Hypersonic flows in thermodynamic and chemical nonequilibrium are investigated for gas mixtures that simulate the air atmosphere. The Navier-Stokes equations are solved including source terms that model the chemical reactions occurring in the present high-enthalpy flows. A two-temperature model is applied to individually account for the translational and rotational modes, and the vibrational and electronic modes. The air flow is considered to be composed of a mixture

of oxygen and nitrogen.

The results demonstrate that, in general, CFD results are able to adequately capture the correct shock stand-off distance along the flow stagnation line, and the behavior of the thermodynamic nonequilibrium properties in terms of temperature modes. In addition, the authors also detail the infrared spectra of radiative heat flux at the cylinder stagnation point using a line-by-line approach obtained with the NEQAIR code. Two different databases were considered, and the results showed that HITRAN presents better resolution in terms of the specific intensity spectra. However, the results are equivalent in terms of scanned spectra. The main objective of the present effort is to increase the understanding of the behavior of thermodynamic properties along the flow stagnation line, as well as to obtain the predominant spectrum of infrared radiation at the flow stagnation point on the cylinder surface.

6. ACKNOWLEDGEMENTS

The authors gratefully acknowledge the support for the present research provided by Conselho Nacional de Desenvolvimento Científico e Tecnológico, CNPq, under the Research Grants No. 309985/2013-7, 304335/2018-5 and 407842/2018-7. The work is also supported by computational resources of the Center for Mathematical Sciences Applied to Industry (CeMEAI), funded by Fundação de Amparo à Pesquisa do Estado de São Paulo, FAPESP, under the Research Grant No. 2013/07375-0. The authors acknowledge the National Laboratory for Scientific Computing, LNCC/MCTI, Brazil, for providing HPC resources of the SDumont supercomputer, under the HFWBTF project, which have contributed to the research results reported in the present paper. FAPESP Research Grant No. 2013/08293-7 is further acknowledged by the authors. Support to the first author under the FAPESP Scholarship Grants No. 2021/02705-8 and 2022/07604-8, and additional support to the fifth author under FAPESP Research Grant No. 2013/07375-0 are also gratefully acknowledged. The research being performed at the University of Illinois at Urbana–Champaign is supported by the United States Air Force Office of Scientific Research through Grant No. FA9550-19-1-0342.

7. REFERENCES

Agarwal, R.K., Yun, K.Y. and Balakrishnan, R., 2001. "Beyond Navier–Stokes: Burnett equations for flows in the continuum-transition regime". *Physics of Fluids*, Vol. 13, No. 10, pp. 3061–3085. doi:10.1063/1.1397256.

Alladadi, F.A., Rongier, I. and Wilde, P.D., 2013. *Safety Design for Space Operations*. Elsevier, Oxford.

Bird, G.A., 1994. *Molecular Gas Dynamics and the Direct Simulation of Gas Flows*. Clarendon Press, Oxford.

Blottner, F.G., Johnson, M. and Ellis, M., 1971. "Chemically reacting viscous flow program for multi-component gas mixtures". Technical report, Sandia Labs.

Bobylev, A.V., 1982. "The Chapman-Enskog and grad methods for solving the Boltzmann equation". *Akademiia Nauk SSSR Doklady*, Vol. 262, No. 1, pp. 71–75. URL `http://mi.mathnet.ru/dan44973`.

Cramer, M.S., 2012. "Numerical estimates for the bulk viscosity of ideal gases". *Physics of Fluids*, Vol. 24, No. 6, pp. 066102.1–066102.23. doi:10.1063/1.4729611.

Cruden, B.A. and Brandis, A.M., 2019. "NEQAIR v15.0 release notes". Technical report, NASA TR 20190032487.

Daniel, K., Jans, E., Lynch, K.P., Swain, W., Downing, C. and Wagner, J.L., 2023. "Nitric oxide emission spectroscopy of a cylinder stagnation flow in a shock tunnel". In AIAA Paper No. 2023-1174*, AIAA SCITECH 2023 Forum*. National Harbor, MD & Online. doi:10.2514/6.2023-1174.

Gillespie, L.J., 1930. "The Gibbs-Dalton law of partial pressures". *Physical Review*, Vol. 36, No. 1, pp. 121–131. doi:10.1103/physrev.36.121.

Gnoffo, P.A., Gupta, R.N. and Shinn, J.L., 1989. "Conservation equations and physical models for hypersonic air flows in thermal and chemical nonequilibrium". Technical report, NASA Report 2867.

Hirsch, C., 2007. *Numerical Computation of Internal and External Flows: The Fundamentals of Computational Fluid Dynamics*. Elsevier, Oxford.

Jawahar, P. and Kamath, H., 2000. "A high-resolution procedure for Euler and Navier–Stokes computations on unstructured grids". *Journal of Computational Physics*, Vol. 164, No. 1, pp. 165–203. doi:10.1006/jcph.2000.6596.

Karpuzcu, I.T., Jouffray, M.P. and Levin, D.A., 2023. "Effect of oxygen dissociation on nitric oxide ultraviolet emissions". *Journal of Thermophysics and Heat Transfer*, Vol. 37, No. 1, pp. 147–160. doi:10.2514/1.T6609.

Li, Z., Sohn, I. and Levin, D., 2012. "DSMC modeling of NO formation for simulation of radiation in hypersonic flows". In AIAA Paper No. 2012-0228*, 50th AIAA Aerospace Sciences Meeting including the New Horizons Forum and Aerospace Exposition*. Nashville, TN. doi:10.2514/6.2012-228.

MacCormack, R.W. and Candler, G.V., 1989. "The solution of the Navier-Stokes equations using Gauss-Seidel line relaxation". *Computers & Fluids*, Vol. 17, No. 1, pp. 135–150. doi:10.1016/0045-7930(89)90012-1.

Martin, A., Scalabrin, L.C. and Boyd, I.D., 2012. "High performance modeling of atmospheric re-entry vehicles". *Journal of Physics: Conference Series*, Vol. 341, No. 1, pp. 012002.1–012002.12. doi:10.1088/1742-6596/341/1/012002.

Modest, M.F., 2003. *Radiative Heat Transfer (2nd edition)*. Academic Press, New York.

Moreira, F.C., Wolf, W.R. and Azevedo, J.L.F., 2021. "Thermal analysis of hypersonic flows of carbon dioxide and air

in thermodynamic non-equilibrium". *International Journal of Heat and Mass Transfer*, Vol. 165, No. Part A, pp. 120670.1–120670.19. ISSN 0017-9310. doi:10.1016/j.ijheatmasstransfer.2020.120670.

Niu, Q., Yuan, Z., Dong, S. and Tan, H., 2018. "Assessment of nonequilibrium air-chemistry models on species formation in hypersonic shock layer". *International Journal of Heat and Mass Transfer*, Vol. 127, No. Part A, pp. 703–716. ISSN 0017-9310. doi:10.1016/j.ijheatmasstransfer.2018.07.007.

Nompelis, I., Candler, G. and Conti, R., 2009. "A parallel implicit CFD code for the simulation of ablating re-entry vehicles". In AIAA Paper No. 2009-1562*, 47th AIAA Aerospace Sciences Meeting including The New Horizons Forum and Aerospace Exposition*. Orlando, FL. doi:10.2514/6.2009-1562.

Park, C., 1988. "Assessment of a two-temperature kinetic model for dissociating and weakly ionizing nitrogen". *Journal of Thermophysics and Heat Transfer*, Vol. 2, No. 1, pp. 8–16. doi:10.2514/3.55.

Park, C., 1989. "Assessment of two-temperature kinetic model for ionizing air". *Journal of Thermophysics and Heat Transfer*, Vol. 3, No. 3, pp. 233–244. doi:10.2514/3.28771.

Park, C., 1993. "Review of chemical-kinetic problems of future NASA missions. I-Earth entries". *Journal of Thermophysics and Heat Transfer*, Vol. 7, No. 3, pp. 385–398. doi:10.2514/3.431.

Rothman, L.S., 2021. "History of the HITRAN database". *Nature Reviews Physics*, Vol. 3, No. 5, pp. 302–304. doi: 10.1038/s42254-021-00309-2.

Scalabrin, L., 2007. *Numerical Simulation of Weakly Ionized Hypersonic Flow Over Reentry Capsules*. Ph.D. thesis, University of Michigan. URL `https://www.proquest.com/docview/304842378`.

Sharma, B. and Kumar, R., 2019. "Estimation of bulk viscosity of dilute gases using a nonequilibrium molecular dynamics approach". *Physical Review E*, Vol. 100, No. 1, pp. 013309.1–013309.15. doi:10.1103/PhysRevE.100.013309.

Steger, J.L. and Warming, R., 1981. "Flux vector splitting of the inviscid gasdynamic equations with application to finite-difference methods". *Journal of Computational Physics*, Vol. 40, No. 2, pp. 263–293. doi:10.1016/0021-9991(81)90210-2.

Venkatakrishnan, V., 1995. "Implicit schemes and parallel computing in unstructured grid CFD". Technical report, NASA CR-195071.

Vincenti, W. and Kruger, C., 1982. *Introduction to Physical Gas Dynamics*. Wiley, New York.

Wilke, C., 1950. "A viscosity equation for gas mixtures". *The Journal of Chemical Physics*, Vol. 18, No. 4, pp. 517–519. doi:10.1063/1.1747673.

Yanes, N.J. and Austin, J.M., 2019. "Nitric oxide spectroscopic measurements in a hypervelocity stagnation flow". In AIAA Paper No. 2019-0794*, AIAA Scitech 2019 Forum*. San Diego, California. doi:10.2514/6.2019-0794.

8. RESPONSIBILITY NOTICE

The authors are solely responsible for the printed material included in this paper.